

## Plastic Crystalline Lithium Salt with Solid State Ionic Conductivity and High Lithium Transport Number

Makoto Moriya, Daiki Kato, Wataru Sakamoto, and Toshinobu Yogo

Lithium bis(trifluoromethanesulfonyl)imide (LiTFSI) and 2-methoxy-methanol were purchased from Tokyo Chemical Industry Co.  $\text{CDCl}_3$  was purchased from Sigma-Aldrich Co. Lithium foil was purchased from The Honjo Chemical Co. These reagents were used as received.  $\text{LiB}(\text{OCH}_3)_4$  was prepared according to a previously published report.<sup>1</sup>

All air- and moisture-sensitive compounds were manipulated using standard Schlenk and vacuum line techniques or treated in a high-integrity argon-filled glove box (LABmaster, MBraun or UN-650F, UNICO).

$^1\text{H}$ ,  $^{11}\text{B}$ , and  $^{13}\text{C}$  NMR spectra were recorded with a JEOL A-400.  $^1\text{H}$  and  $^{13}\text{C}$  NMR spectra were referenced to the natural-abundance proton or carbon signal of the solvent employed.  $^{11}\text{B}$  NMR spectra were referenced to the boron trifluoride-ethyl ether complex as an external standard. TG-DTA analyses were performed with Rigaku, Thermoplus Evo with a heating rate of  $10\text{ }^\circ\text{C}/\text{min}$  in  $\text{O}_2$  using  $\text{Al}_2\text{O}_3$  as a reference. DSC analyses were performed with SII, EXSTAR DSC6220 with a heating rate of  $10\text{ }^\circ\text{C}/\text{min}$  in  $\text{N}_2$  using  $\text{Al}_2\text{O}_3$  as a reference. Melting points were determined using the derivative of DSC curve combined with the extrapolation method. FAB-MS was recorded on a JEOL, JMS-700. Elemental analysis was performed on a Perkin Elmer 2400II.

Ionic conductivities were measured using the disks of electrolyte sandwiched between two SUS plates in a two electrode cell and sealed in a closed vessel. The vessel was placed into a bench-top type temperature chamber (ESPEC, SU-241). Conductivity data were collected by AC impedance measurements with a Solartron 1260 frequency response analyzer. The transport numbers were determined according to a previously published report using lithium foil as a non-blocking electrode.<sup>13</sup> All cells for electrochemical experiments were assembled in a glove box and equilibrated at the operating temperature for at least 3 h before taking any measurements.

Synthesis of **1**:  $[\text{LiB}(\text{OCH}_3)_4]$  (797.9 mg, 5.68 mmol) and 2-methoxy-methanol (4 mL) were charged in a reaction flask. The solution was refluxed under nitrogen atmosphere for 24 h. After the removal of solvent under reduced pressure, the resulting solid was purified by recrystallization using hot acetonitrile as a crystallization solvent to give  $[\text{LiB}(\text{OCH}_2\text{CH}_2\text{OCH}_3)_4]$  (1293 mg, 4.06 mmol, 71 %) as a white solid.  $^1\text{H}$  NMR (400 MHz,  $23\text{ }^\circ\text{C}$ ,  $\text{CDCl}_3$ )  $\delta$ : 3.52 (t,  $J_{\text{HH}} = \text{Hz}$ , 2H,  $\text{CH}_2$ ), 3.44 (t,  $J_{\text{HH}} = \text{Hz}$ , 2H,  $\text{CH}_2$ ), 3.31 (s, 3H,  $\text{CH}_3$ ).  $^{13}\text{C}$  NMR (100 MHz,  $23\text{ }^\circ\text{C}$ ,  $\text{CDCl}_3$ )  $\delta$ : 74.2 ( $\text{CH}_2$ ), 59.6 ( $\text{CH}_2$ ), 58.7 ( $\text{CH}_3$ ).  $^{11}\text{B}$  NMR (128 MHz,  $23\text{ }^\circ\text{C}$ ,  $\text{CDCl}_3$ ) 2.6 (s). Anal. Calcd for  $\text{C}_{12}\text{H}_{28}\text{BLiO}_8$ : C, 45.31; H, 8.87. Found: C, 43.34; H, 9.75. Owing to the highly hygroscopic nature of **1**, elemental analysis of the compound did not show very good agreement with calculated value. FAB-MS (neg). Calcd for  $\text{C}_{12}\text{H}_{28}\text{BO}_8^-$ : 311, Found: 311.

Lithium borate **1** was purified by recrystallization from hot acetonitrile solution at least three times followed by drying under reduced pressure for a few days. We confirmed the absence of the signals attributable to water, methanol, and acetonitrile from the  $^1\text{H}$  and  $^{13}\text{C}$  NMR spectra of **1**. This result supports the high purity of the borate **1**. Moreover, to support the purity, thermogravimetry (TG) analysis of **1** was performed. The obtained TG curve of **1** did not show practical weight loss from 21 to  $100\text{ }^\circ\text{C}$ . The results shown in Figs. S13 and S14 indicate that the borate **1** is not contaminated by water or solvent. The endothermic peak at around  $65\text{ }^\circ\text{C}$  in the DTA curve corresponds to the phase transition from crystal to plastic crystal. Borate **1** dissolved in  $\text{DMSO}-d_6$  gradually decomposed into boric acid and 2-methoxyethanol under air as a result of hydrolysis a few days after NMR measurements. Therefore, borate **1** should be handled under inert atmosphere.

1 J. Barthel, R. Buestrich, E. Carl, H. J. Gores, *J. Electrochem. Soc.*, 1996, **143**, 3572.



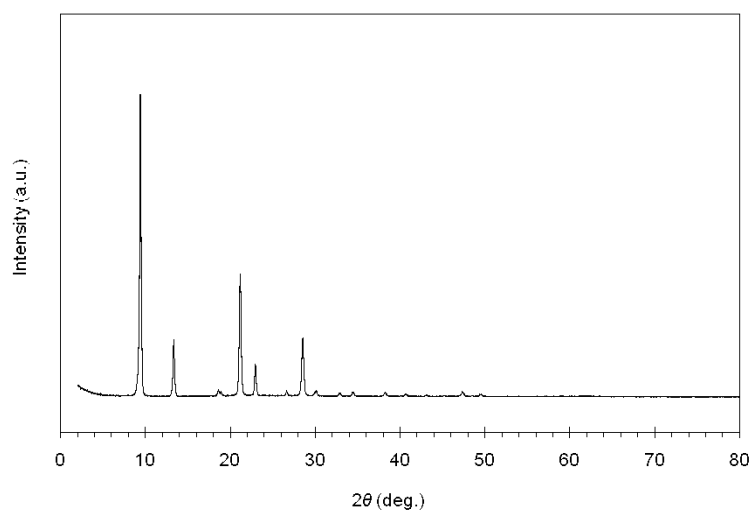


Figure S1. XRD Pattern of **1** measured at ambient temperature.

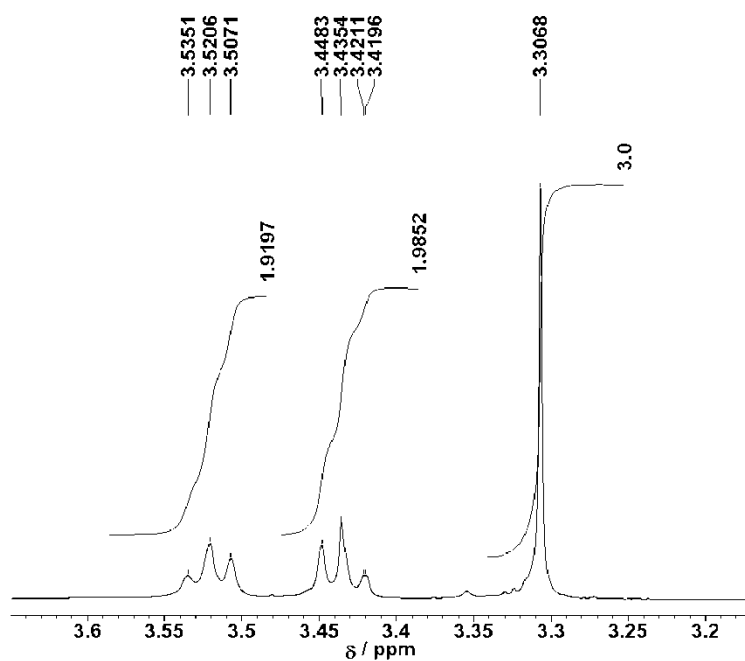


Figure S2. <sup>1</sup>H NMR spectrum of **1**.

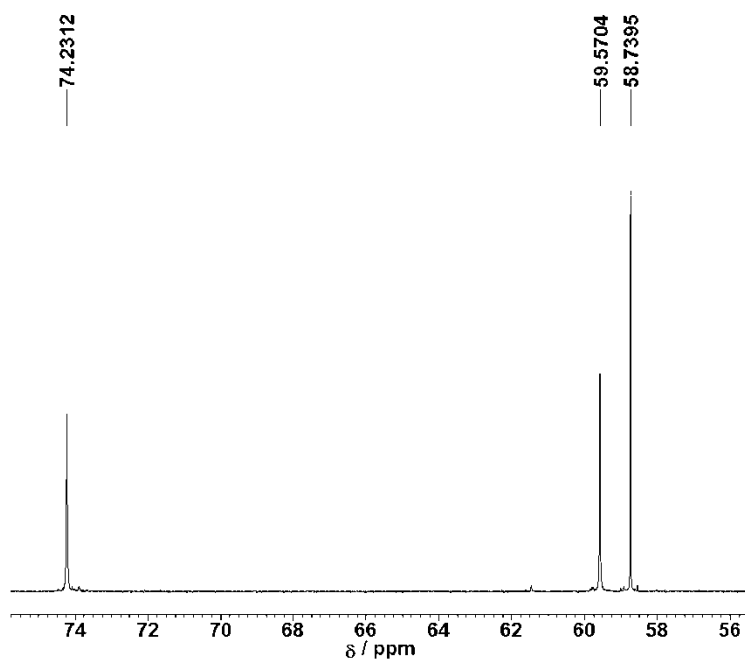


Figure S3.  $^{13}\text{C}$  NMR spectrum of **1**.

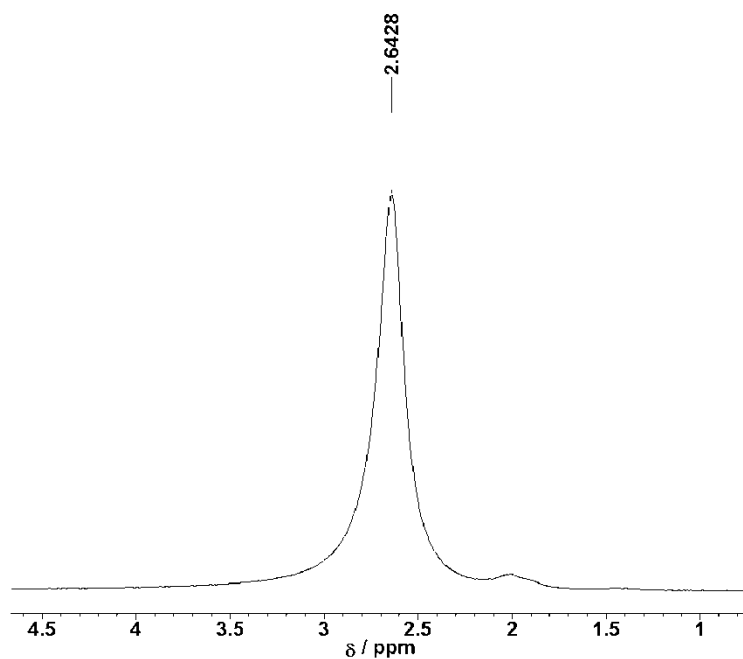


Figure S4.  $^{11}\text{B}$  NMR spectrum of **1**.

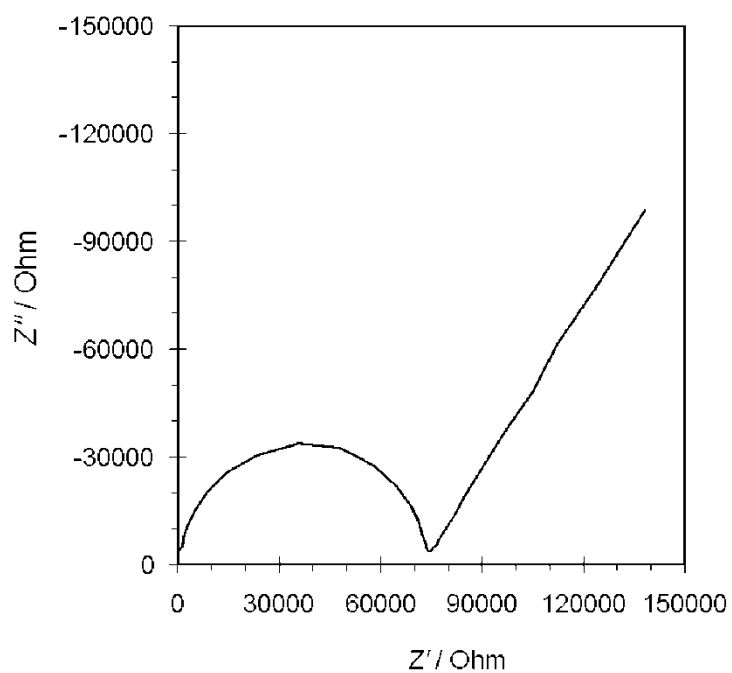


Figure S5. Complex impedance plot of **1**-0.5 at 50 °C. Similar plots were obtained for all the electrolytes reported here.

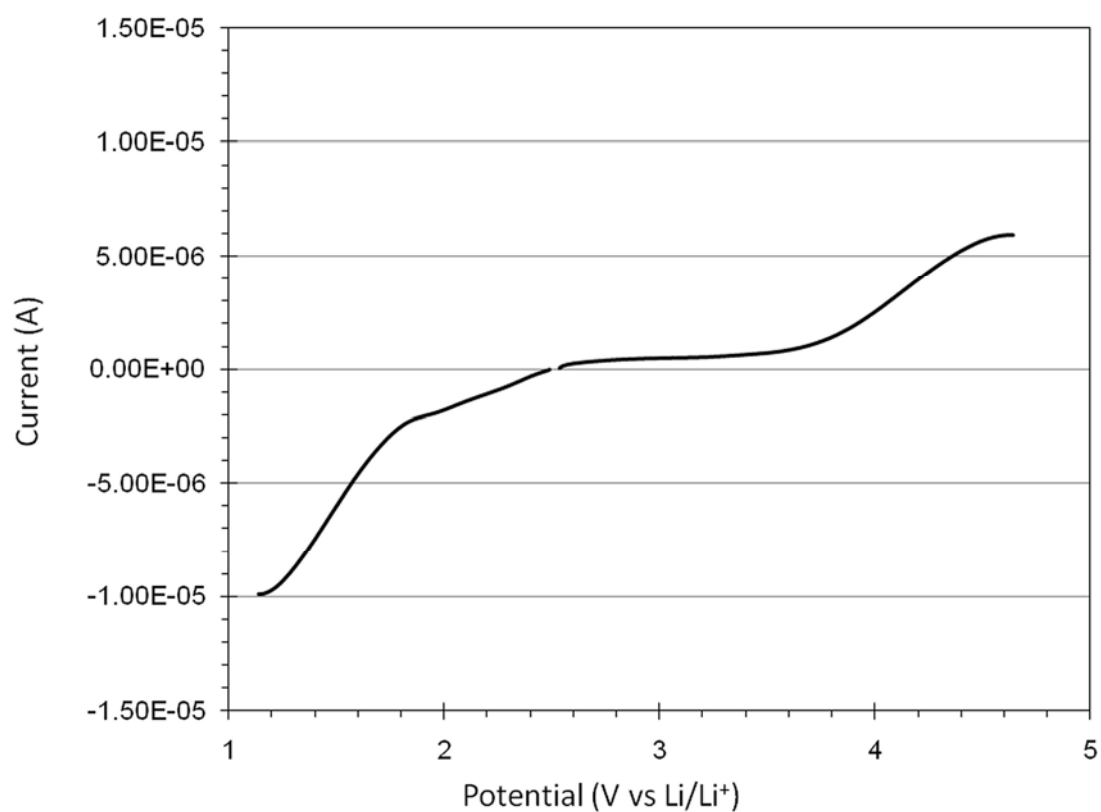


Figure S6. Linear sweep voltammogram of **1**-0.1 at 80 °C with a scan rate of 1mV s<sup>-1</sup>. Stainless steel working electrode

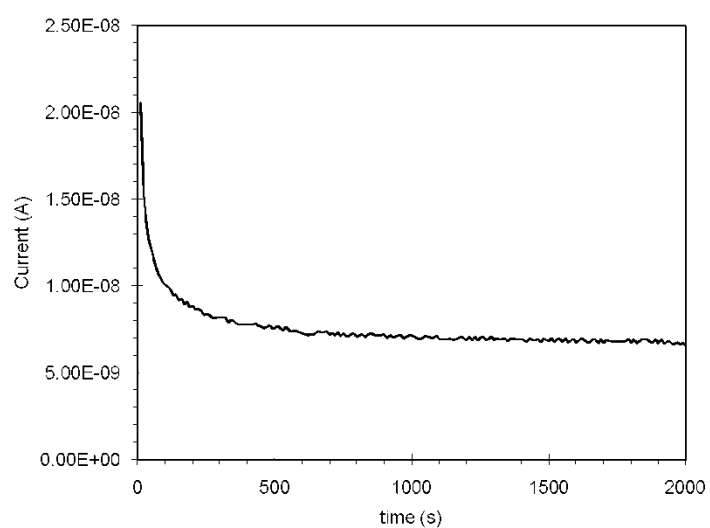


Figure S7. The dc current of **1** as a function of time at 80°C.

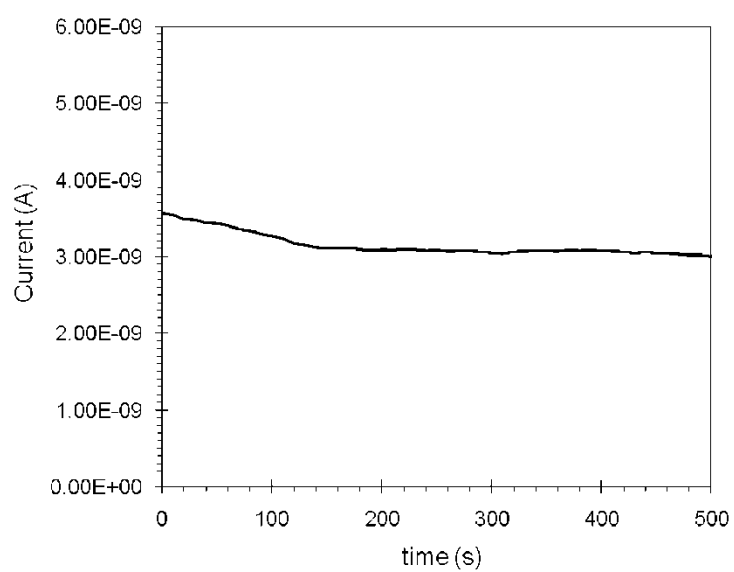


Figure S8. The dc current of **1-0.1** as a function of time at 40°C.

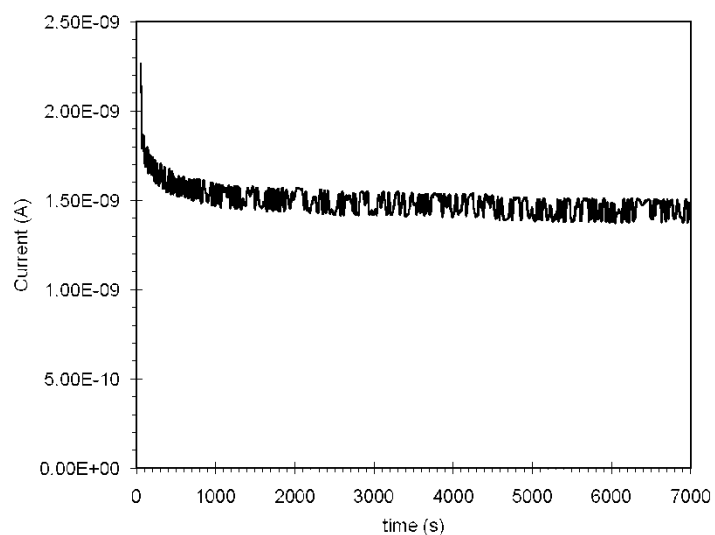


Figure S9. The dc current of **1**-0.5 as a function of time at 40°C.

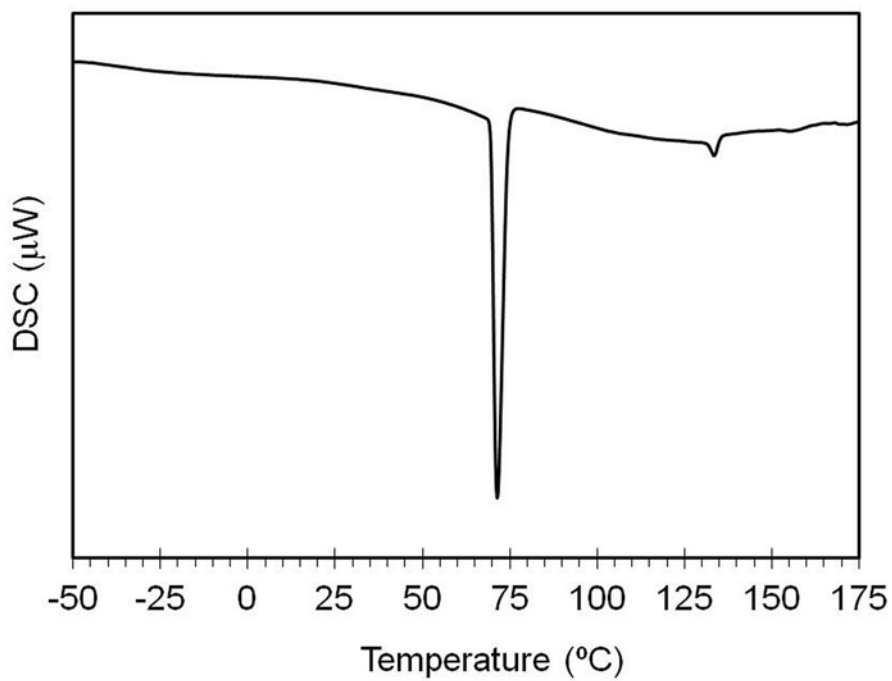


Figure S10. DSC curve of **1**-0.1.

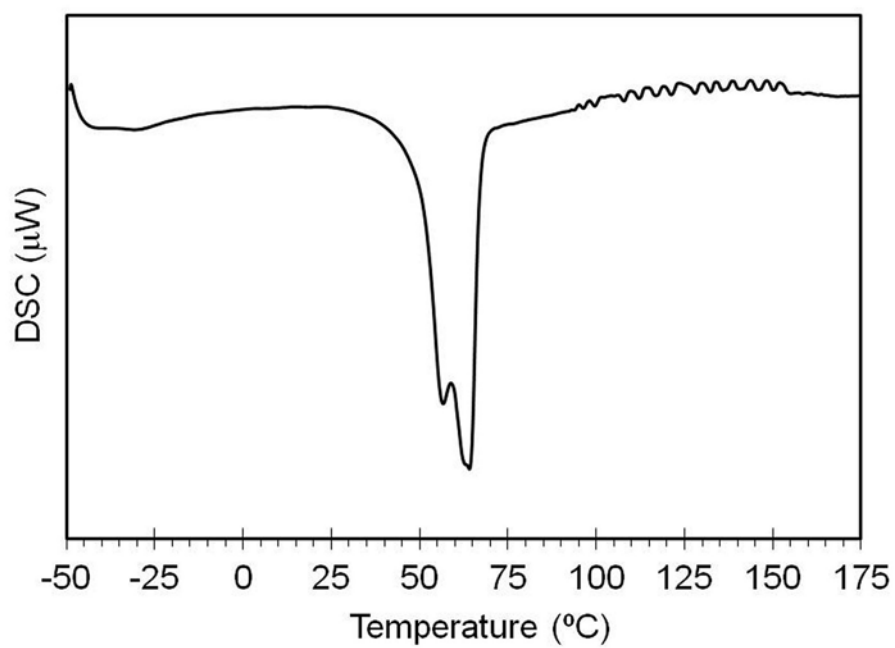


Figure S11. DSC curve of **1**-0.5.

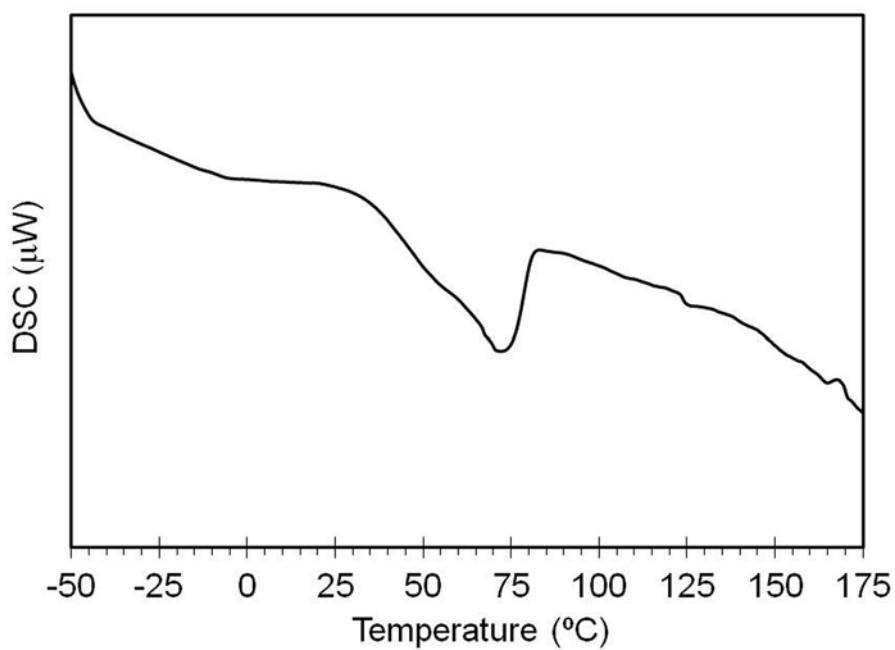


Figure S12. DSC curve of **1**-1.0.



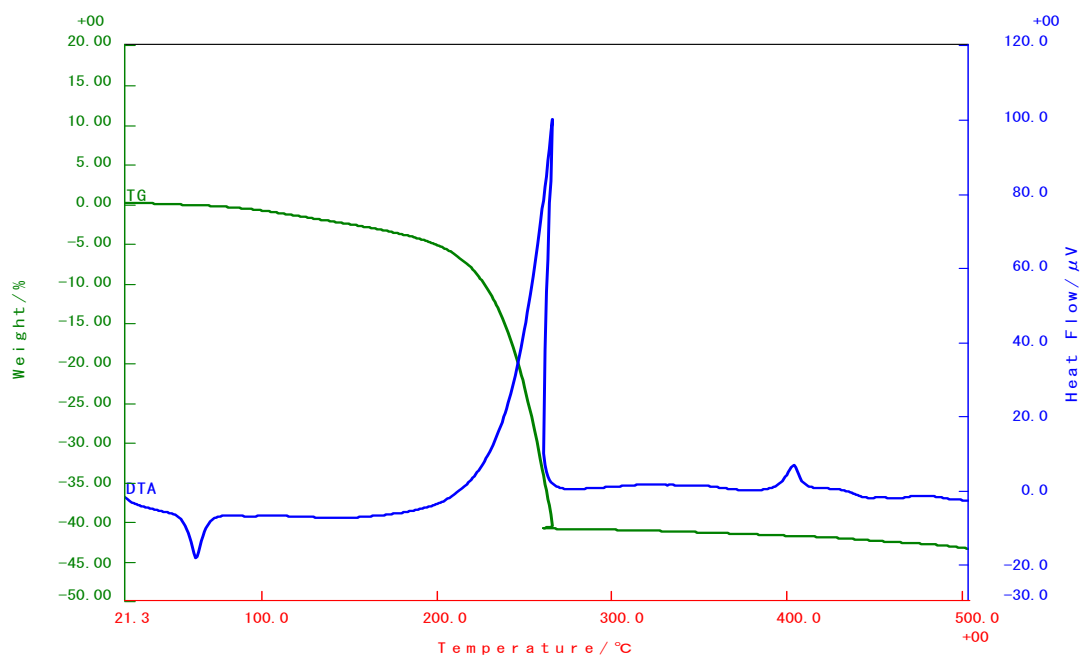


Figure S13. TG-DTA curves of **1**.

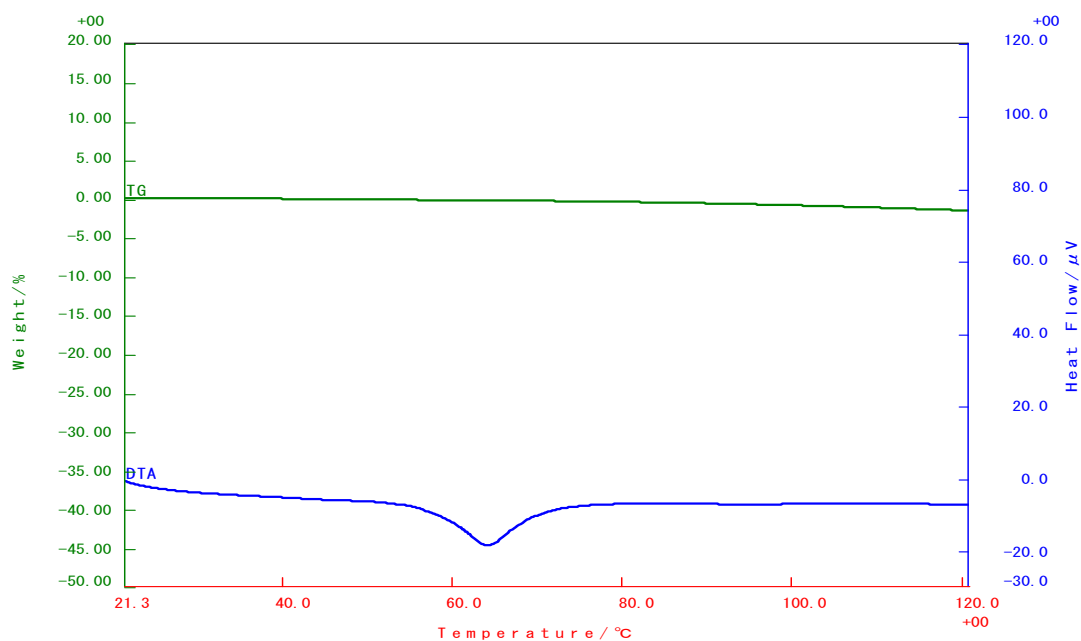


Figure S14. Magnified region of TG-DTA curves of **1** from 21 to 120 °C.